THE UNIVERSITY OF OKLAHOMA

GRADUATE COLLEGE

APPROXIMATIONS TO THE ELECTRIC MICROFIELD DISTRIBUTION FUNCTION IN IONIZED GASES

A DISSERTATION

SUBMITTED TO THE GRADUATE FACULTY

in partial fulfillment of the requirements for the

degree of

DOCTOR OF PHILOSOPHY

BY

HORACE E. HOFFMAN

Norman, Oklahoma

1958

APPROXIMATIONS TO THE ELECTRIC MICROFIELD DISTRIBUTION

FUNCTION IN IONIZED GASES

APPROVED BY

R. G. Fowler

J. Rud Nielsen

Arthur Bernhart

DISSERTATION COMMITTEE

ACKNOWLEDGEMENTS

The author wishes to express his gratitude to Dr. R. G. Fowler for suggesting a study of this problem and to Dr. O. H. Theimer for the advice and innumerable proposals which have made its completion possible. He also gratefully acknowledges the invaluable help and encouragement of his wife, Mary.

This work has been supported in part through a grant sponsored by the National Science Foundation.

TABLE OF CONTENTS

Page

LIST OF TABLES v

LIST OF ILLUSTRATIONS vi

INTRODUCTION 1

Chapter

I. APPLICATIONS OF THE DEBYE-HUCKEL THEORY TO THE ELECTRIC MICROFIELD 7

II. NEAREST NEIGHBOR APPROXIMATION AND THE MARKOFF METHOD OF SUMMATION 15

III. THE LIMIT AND INTEGRATION OF THE FUNCTION $G_N(\rho)$ 27

IV. THE ASSOCIATED MICROFIELD DISTRIBUTION $H(\beta)$ IN THE SHIELDED FORCE APPROXIMATION 42

BIBLIOGRAPHY 49

APPENDIX 51

LIST OF TABLES

Table Page

I. The Debye Shielding Constant κ_T 9

LIST OF FIGURES

Figure		Page
1.	The Holtsmark Electric Field Probability Function	4
2.	$H(\beta)$ in the Nearest Neighbor Approximation	19
3.	Nomograph for $X(\eta)$	32
4.	The Integrand I Represented as a Function of η	33
5.	Upper and Lower Limit of the Function $X_g^3(\eta)$	41
6.	The Integrand of the Function $H(\beta)$	44
7.	The Distribution Function $H(\beta)$	46

APPROXIMATIONS TO THE ELECTRIC MICROFIELD DISTRIBUTION FUNCTION IN IONIZED GASES

INTRODUCTION

The behavior of ionized gases can best be predicted if the microfield within the plasma is known. For instance, the Stark theory of line broadening by the microfield permits concentration determinations, and the evaluation of transport coefficients of viscosity and electrical conductivity is completed through knowledge of the scattering micro-potential and its gradient.[1,2] An examination of current statistical theories reveals two defects which will admit the modification presented in this paper.

Consider a volume V occupied by an assembly of N electrical systems, e.g., ions, in thermal equilibrium. At an arbitrary point O within V let us ask for both the instantaneous magnitude of the electrical field $\vec{E}_0$, and its time variant fluctuation. If we temporarily ignore the thermal motion of the ensemble members, a given configuration of the swarm of electrical perturbers produces a definite microfield at O. However, a greater number of configurations may be compatible with this microfield for one value of $\vec{E}_0$ than for another. In the absence of a configuration

---

[1]S. Chandrasekhar, Astrophys. J., 97, 255 (1943).

[2]L. Spitzer and R. Harm, Phys. Rev., 89, 977 (1953).

specification one can calculate only a distribution of $\vec{E}_o$ at O. If each member is permitted its thermal activity one now calculates the variation of $\vec{E}_o$ in time due to the random motions of the perturbers. Probability after-effects encountered in such calculations were first studied by Smoluchowski[1] and have more recently been investigated by Chandrasekhar and von Neumann.[2] Over long time intervals one expects no correlation of microfield values at O, since the stationary distribution, computed by assumming immobility, represents the time average of $\vec{E}_o$. But if one is interested in observations at O over small time intervals an analysis of the time variation of source configurations is indicated. We examine only the time averaged microfield, and let $W(\vec{E}_o)d\vec{E}_o$ represent the probability that the electric field at a point O possesses a value $\vec{E}$ such that for its components X, Y and Z

1. $$X_o - 1/2\ dX_o \leq X \leq X_o + 1/2\ dX_o, \text{ etc.}$$

Alternatively we shall express this and similar inequalities by saying $\vec{E}$ lies in the interval $d\vec{E}_o$ about $\vec{E}_o$. The following outline of the most successful method for evaluation of $W(\vec{E}_o)$ is due to Holtsmark.[3]

In 1919, prompted by the then recent experiments of Fuchtbauer and Hoffmann[4] on the shift and splitting of spectral lines, Holtsmark calculated the probability distribution of the strength of the field produced by a static random distribution of either ions, dipoles or

---

[1] M. Smoluchowski, Wien. Ber. 124, 339 (1915).

[2] S. Chandrasekhar and J. von Neumann, Astrophys. J. 97, 1 (1943).

[3] J. Holtsmark, Ann. Physik 58, 577 (1919).

[4] C. Fuchtbauer and U. W. Hoffmann, Ann. Physik 43, 96 (1914).

quadrupoles. We are interested only in ions and will omit a review of dipole and quadrupole interactions. Holtsmark's model consisted of an assembly of N identical non-interacting "ions" of valence Z_j, electronic charge ϵ, in position $\vec{r}_j$; each contributing to the microfield at 0 a vectorial component

2. $$\vec{E}_j = (ez_j/r_j^3)\ \vec{r}_j \ ;$$

the total field fluctuating subject to the condition of constant mean density n, equal to N/V. The total field at 0 is given by

3. $$\vec{E} = \sum_{j=1}^{N} \vec{E}_j(\vec{r}_j).$$

Since the particles were assumed non-interacting, he wrote for the probability that $\vec{r}_j$ lay in the interval $d\vec{r}_j$ about $\vec{r}_j$

4. $$\sigma_j(x_j,y_j,z_j)dx_j dy_j dz_j = \sigma_j(\vec{r}_j)d\vec{r}_j = d\vec{r}_j/V.$$

His analytic formulation of the problem was to sum

5. $$W_N(\vec{E}_o)d\vec{E}_o = 1/V^N \int \underset{3N}{\cdots} \int \prod_{j=1}^{N} d\vec{r}_j$$

over a range of integration including only those volume elements compatible with the condition that $\vec{E}$ lay in the interval $d\vec{E}_o$ about $\vec{E}_o$. To facilitate numerical calculation and graphical representation, Holtsmark put

6. $$E_o = E_n \beta = 2.61\epsilon n^{+2/3} \beta \ ,$$

and expressed the distribution of the absolute value of the microfield in terms of β as

7. $$W(E_o)dE_o = W(\beta)d\beta \ .$$

His result is given in Figure 1. From it he computed the intensity of

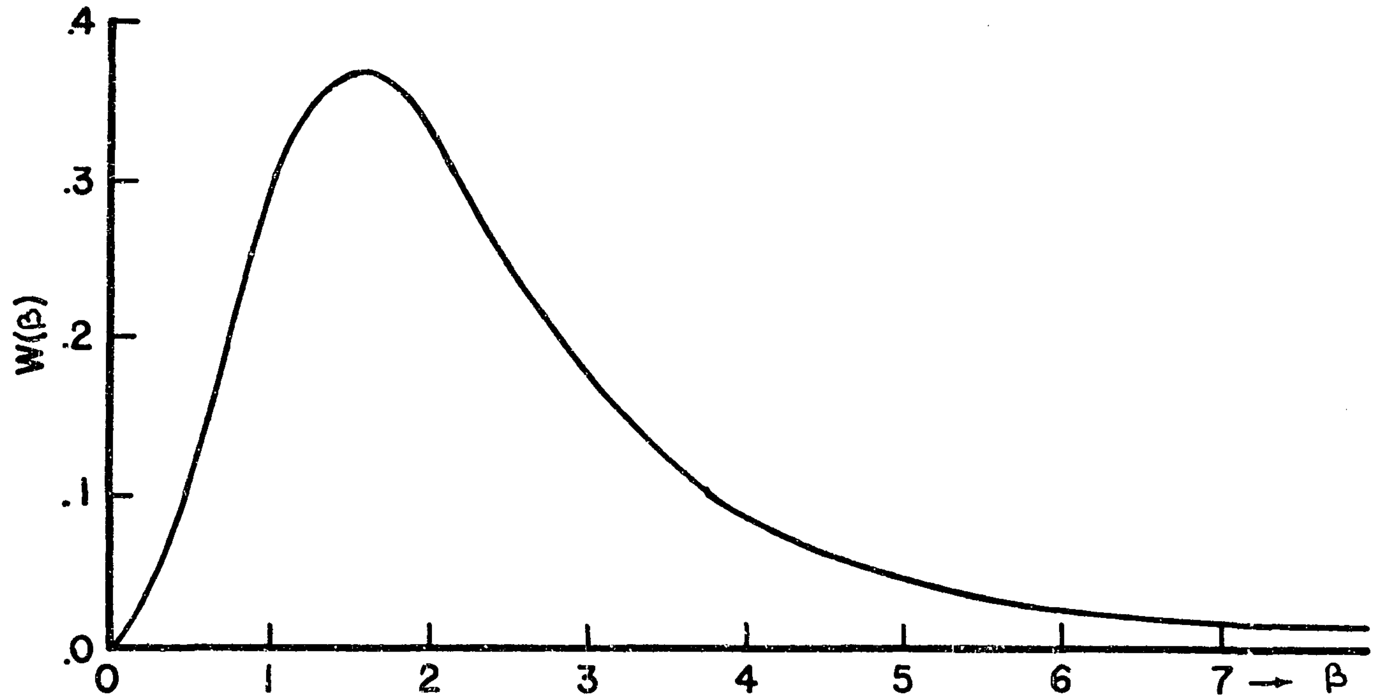

FIGURE 1 -- HOLTSMARK ELECTRIC FIELD PROBABILITY FUNCTION

spectral lines of hydrogen as a function of radiation frequency.

The experimental confirmation of Holtsmark's theory of line broadening has not been satisfactory. Many investigators[1,2,3] have compared theoretical profiles with those obtained in a variety of experiments and found substantial disagreement; while experiments at the University of Oklahoma[4,5,6] have led to a further discrepancy. Both the theory of Holtsmark and the Hall[7] effect were utilized to measure ion concentration in shock induced plasmas as a function of distance along the shock tube axis. Calculations based on the Hall effect indicated a monotonic decrease of concentration with shock progress, while calculations employing the theory of Holtsmark indicate the existence of a concentration maximum in the neighborhood of the axis center.

Recent modifications of the theory of line broadening have centered about the time dependence of the microfield. Intensity variations are considered the consequence of velocity or collision broaden-

---

[1]L. H. Aller, Astrophy. J., 96, 321 (1942).

[2]H. Griem, Z. Physik., 137, 280 (1954).

[3]E. B. Turner and L. Doherty, Astron. J., 60, 158 (1955).

[4]R. G. Fowler, W. R. Atkinson and L. W. Marks, Phys. Rev., 87, 966 (1952).

[5]W. R. Atkinson, "Half Intensity Breadths of the Balmer Lines in Pulsed Gas Discharges" (unpublished M. S. thesis, University of Oklahoma, 1950).

[6]B. E. Clotfelter, "Experimental Studies of Transport Phenomena in Highly Ionized Gases" (unpublished Ph. D. dissertation, University of Oklahoma, 1953).

[7]E. H. Hall, Am. Jour. of Math., 2, 287 (1879).

ing by electrons, and quantum theoretical calculations are employed to determine transition probabilities.[1,2,3,4] As none of these theories have been decisive, and the latest, most successful investigation[5] depends for its development upon the stationary microfield distribution, it is desirable to seek a corrective modification of Holtsmark's theory. Our starting point is the observation that a single kind of non-interacting monopole as a field source constitutes a physically unrealistic assumption. Any ionized gas must consist of at least two species of interacting monopoles, and the consequence of this fact for the microfield distribution will be developed in this thesis.

---

[1]J. H. Van Vleck and V. F. Weisskopf, Rev. Mod. Phys., 17, 227 (1945).

[2]M. K. Krogdahl, Astrophys. J., 110, 355 (1945).

[3]B. Kivel, S. Bloom, and H. Margenau, Phys. Rev., 98, 495 (1955).

[4]A. C. Kolb, ASTIA Document No. AD115040, University of Michigan, Eng. Res. Inst. (1957).

[5]*Ibid.*

CHAPTER I

APPLICATIONS OF THE DEBYE-HUCKEL THEORY TO THE ELECTRIC MICROFIELD

1. Preliminary Remarks

If a Coulomb law of force is associated with each interacting particle it is difficult to determine for N values of j, the probability distribution that all N particles simultaneously lie in their respective neighborhoods $d\vec{r}_j$ about $\vec{r}_j$. However, this calculation may be avoided by making use of principles first introduced by Debye.[1] One may choose a particular particle of an assembly and compute the mean potential, $\psi(r)$, in the atmosphere surrounding it. This potential is contributed by the select particle at the center and the charge cloud formed by the remaining members (see Section 2), while its gradient is regarded as the field associated with the central particle. The probability density for this configuration then may be shown to be the volume reciprocal, 1/V. We review here the treatment of Debye which has been verified by Fowler,[2] and Kramers[3] using strict statistical mechanics.

---

[1] P. Debye and E. Hückel, Phys. Z., 24, (1923).

[2] R. H. Fowler, Proc. Camb. Phil. Soc., 22, 861 (1925).

[3] H. A. Kramers, Proc. Amsterdam, 30, 145 (1927).

2. The Ionic Atmosphere and Associated Potential of a Point Charge

Let a spherical plasma volume V contain s species of monopole; taking the valence, total number and average particle density of the i^{th} species as Z_i, N_i and n_i respectively. Then if N denotes the total number of particles corresponding to an average particle density n,

12.1 $$n = N/V = \sum_{i=1}^{s} N_i/V = \sum_{i=1}^{s} n_i \, .$$

The valence z_i may be positive or negative; the dielectric constant of the plasma is taken as unity; while ϵ represents the value of electronic charge (i.e., 4.8×10^{-10} e.s.u.). Focusing our attention upon a point O at fixed distance r from a particular ion, we require the mean potential $\psi(r)$ at this point.

According to Boltzmann's theorem, in a small element of volume dV surrounding O, the number of the i^{th} ionic species is given by

12.2 $$n_i \exp(-\epsilon z_i \psi/kT) \, dV.$$

Assuming isotropy of the plasma and neglecting boundary effects, a radial charge density function, $\mu(r)$, about the central monopole is then described by

12.3 $$\mu(r) = \epsilon \sum_{i=1}^{s} z_i n_i \exp(-\epsilon z_i \psi/kT) \; ;$$

where

12.4 $$\epsilon \sum_{i=1}^{s} n_i z_i = 0 \, .$$

Of course, $\mu(r)$ represents the local time average charge density about the central ion. This is usually referred to as the Debye charge cloud. Since the probability for approach of particles of opposite sign is greater than for those of like sign, the temporal mean over near neighborhoods of a given point charge should yield a net negative density for positive charge centers and positive density for negative centers.

The solution for $\psi(r)$ is effected through Poisson's equation for $\psi(r)$;

12.5 $$\nabla^2\psi = 4\pi\rho = 4\pi\epsilon \sum_{i=1}^{s} n_i z_i \exp(-\epsilon z_i \psi/KT).$$

In order to put equation (12.5) in more tractable form the exponentials may be expanded; retaining terms only to first order one obtains

12.6 $$\nabla^2\psi = \kappa^2\psi,$$

where

12.7 $$\kappa^2 = (4\pi\epsilon^2/KT) \sum_{i=1}^{s} n_i z_i^2 .$$

The most general spherically symmetrical solution to (12.6) is

12.8 $$\psi(r) = (A/r)\exp(-\kappa r) + (B/r)\exp(\kappa r),$$

and since $\psi(r)$ must vanish for infinite values of r, B must vanish. With a j^{th} species as charge center, the condition that

12.9 $$\lim_{r\to 0} \psi(r) = z_j\epsilon/r$$

implies that A is equal to $z_j\epsilon$.

From these results the following set of equations may be collected for future reference:

12.10 $$\rho(r) = (\kappa^2\epsilon z_j/4\pi r)\exp(-\kappa r) ,$$

12.11 $$\psi = \psi_1 + \psi_2 = (\epsilon z_j/r) - (\epsilon z_j/r)\left[1-\exp(-\kappa r)\right] = (\epsilon z_j/r)\exp(-\kappa r),$$

12.12 $$\vec{E}(r) = \nabla\psi(r) = (\epsilon z_j/r^3)(1+\kappa r)\exp(-\kappa r)\vec{r} ,$$

12.13 $$\kappa^2 = (4\pi\epsilon^2/kT) \sum_{i=1}^{s} n_i z_i^2 .$$

Thus, the neighborhood of a given point charge is exposed to the field of two sources: the field of the central charge and an additional field being contributed by the remaining charges which generally opposes the field of the center. The net effect is equivalent to a potential with cut-off, the range being determined by Debye's shielding constant κ (see equation 12.11 and 12.13). Numerical values of κ for a variety of temperatures and densities are given in Table 1.

TABLE 1

THE DEBYE SHIELDING CONSTANT κ_T*

n (ions/cc)	κ_T T 24,000	κ_T T 12,000	κ_T T 6,000	κ_T T 2,000
10^{15}	$4.30\ 10^4$	$6.10\ 10^4$	$8.60\ 10^4$	$1.49\ 10^5$
10^{16}	$1.36\ 10^5$	$1.93\ 10^5$	$2.72\ 10^5$	$4.71\ 10^5$
10^{17}	$4.30\ 10^5$	$6.10\ 10^5$	$8.60\ 10^5$	$1.49\ 10^6$
10^{18}	$1.36\ 10^6$	$1.93\ 10^6$	$2.72\ 10^6$	$4.71\ 10^6$
10^{19}	$4.30\ 10^6$	$6.10\ 10^6$	$8.60\ 10^6$	$1.49\ 10^7$
10^{20}	$1.36\ 10^7$	$1.93\ 10^7$	$2.72\ 10^7$	$4.71\ 10^7$

* κ_T denotes the values of κ in reciprocal centimeters at the indicated temperature T degrees Kelvin; and at particle concentration n.

3. The Charge Cloud and the Probability Density of an Ion in Its Role as Cloud Center

The charge cloud is, of course, a statistical concept and represents an average over those configurations of the point charges which have practically the same internal energy and give similar contributions to the microfield $\vec{E}_0$. Each charge is the center of its own companion cloud formed by all the remaining charges, and is a member of all remaining clouds as well. In a plasma having, by definition,[1] macroscopic dimensions

$$L_i \geq 1/\kappa , \qquad (i = 1,2,3)$$

the form and energy of a cloud may be assumed to be independent of the position of its center.

Thus if one studies a point charge in its role as a cloud center, the probability for finding it in a volume element $d\vec{r}$ centered at $\vec{r}$ is proportional to $d\vec{r}$ and is independent of the location $\vec{r}$ of the volume element. Futhermore, it does not depend upon the configuration of the other charges which will always form a cloud compatible with equations (12.10) and (12.11). Contrariwise, if one interprets the same point charge as a member of a cloud about some other center, the probability depends upon the sign of the charge and its distance from the center. Hence, if $\sigma_j(r_j)$ denotes the normalized probability density that the j^{th} charge is located within a volume element $d\vec{r}_j$ about $\vec{r}_j$ and is regarded as the center of a charge cloud, then it has a constant value C and one may write formally

---

[1] I. Langmuir, Phys. Rev., 33, 954 (1929).

$$\int_V \sigma_j(r_j)dr_j = \int_V C dr_j = CV = 1 \quad ; \tag{13.1}$$

so that

$$\sigma_j(r_j) = 1/V \tag{13.2}$$

For emphasis, we repeat that in its role as charge center with the corresponding probability density (13.2), one must associate with the electric center a microfield contribution given by (12.12). The considerations are important when applying Holtsmark's method to a system of interacting particles for which the method is not applicable without modification.

Since the mass of the point charge does not appear in formula (12.13), this formula should be valid for both ions and electrons. It is, however, possible that, in a higher approximation, κ is smaller for electrons than for ions, as the polarization of the plasma may not completely follow the fast movements of the electrons. The following argument indicates that this relaxation effect is actually not very serious. The polarization of the plasma is accomplished by displacements (from random motion) of ions and electrons as well. The latter will respond even to rapid fluctuations of the microfield, the former will not. However, the ions force the electrons to move in bent orbitals, thus producing a correlation between the motion of the electrons and their companion clouds.

4. Two Approximations to the Microfield Employing Debye's Theory of the Polarized Plasma

With the help of Debye's charge cloud, the microfield in a plasma may be treated by two approximations. In the first of these, the electrical potential $\psi(r)$ and its corresponding gradient $\vec{E}(r)$ is given by equations (12.11), and (12.12) respectively. Furthermore, the probability that a site O is exposed to the field $\vec{E}(r)$ is considered equal to the probability that O is at a distance r from the nearest charge. This is the nearest neighbor approximation and it will be fully discussed in the next chapter. Since equation (12.12) is statistical in character, taking into account the average effect of many interacting systems, and since a shielded force has much shorter range than the ordinary Coulomb force, the nearest neighbor approximation is much more appropriate when working with the former force than would be the case for the latter.

The nearest neighbor theory fails when r is large; i.e., when the point O is nearly equidistant from several field producing charges. In this case one has to acknowledge the dual role of a point charge in a plasma, according to which <u>each</u> point charge is not only a member of a shielding cloud, but is also a central source of shielded force. Hence, the microfield may be taken as the vector sum of the shielded fields produced by each and every point charge:

$$\vec{E} = \sum_{j=1}^{N} \vec{F}_j(r_j) = \epsilon \sum_{j=1}^{N} \frac{z_j(1+\kappa r_j)}{r_j^3} \exp(-\kappa r_j)\vec{r}_j \; . \tag{14.1}$$

For binary monovalent systems (the only case considered in the following work) $2N^+$ is equal to N, and

$$\begin{aligned} z_j &= +1 \quad \text{whenever} \quad 1 \leq j \leq N^+ \; , \\ z_j &= -1 \quad \text{whenever} \quad N^+ \leq j \leq N \; . \end{aligned} \tag{14.2}$$

Equation (14.1) is the basis for what will be termed the shielded force approximation to the microfield. Here, as in Holtsmark's theory, the only variables are the $\vec{r}_j$. But one has to realize that the special form of the shielded force (12.12) and the magnitude of the shielding constant (12.13) represent only an average behavior of the plasma. Consistent with the program discussed in the introduction, fluctuations of the analytical form of the shielded force, in particular of κ , are neglected in all of our considerations.

CHAPTER II

THE NEAREST NEIGHBOR APPROXIMATION AND THE MARKOFF METHOD OF SUMMATION

1. The Derivation of the Nearest Neighbor Distribution w(r)

The law of distribution of the nearest neighbor in a random distribution of systems was first considered by Hertz[1] and subsequently was presented in the following form by Chandrasekhar.[2] Let $w(r)dr$ denote the probability that the nearest neighbor to a point O lies in a spherical shell of thickness dr at radial distance r from O. This probability must be equal to the probability that all particles are exterior to the sphere of radius r, times the probability that at least one particle is contained in the spherical shell. Hence $w(r)$ must satisfy the equation

$$21.1 \qquad w(r) = \left[1 - \int_0^r w(r)dr\right] 4\pi r^2 n,$$

where n denotes the constant average number of particles per unit volume. From equation (21.1) we derive

$$21.2 \qquad \frac{d}{dr}\left[\frac{w(r)}{4\pi r^2 n}\right] = -4\pi r^2 n \left[\frac{w(r)}{4\pi r^2 n}\right].$$

The solution to (21.2) is given by

---

[1] P. Hertz, Math. Ann., 67, 387 (1909).

[2] S. Chandrasekhar, Rev. Mod. Phys., 15, 87 (1943).

21.3 $$w(r) = 4\pi r^2 n \exp\left(-\frac{4\pi r^3 n}{3}\right) ,$$

since according to (21.1),

21.4 $$w(r) \to 4\pi r^2 n \quad \text{as } r \to 0.$$

For a large number of particles $N \gg 1$, using the distribution (21.3), an exact formula for the average distance, $\langle r \rangle$, between particles may be derived.

By definition

21.5 $$\langle r \rangle = \int_0^\infty r w(r) dr = 4\pi n \int_0^\infty r^3 \exp\left(-\frac{4\pi r^3 n}{3}\right) dr,$$

and with suitable substitutions equation (21.5) reduces to

21.6 $$\langle r \rangle = \left(\frac{3}{4\pi n}\right)^{1/3} \int_0^\infty x^{1/3} \exp(-x) dx = \Gamma(4/3) \left(\frac{3}{4\pi n}\right)^{1/3} = 0.554 n^{-1/3} .$$

This value may be contrasted to that defined in the literature[1] by the relation

21.7 $$4\pi \langle r \rangle^3 n/3 = 1 ;$$

so that

21.8 $$\langle r \rangle = (3/4\pi n)^{1/3} = 0.621 n^{-1/3} .$$

However, to facilitate comparisons, we shall use definition (21.7) in subsequent work. According to the discussion of Chapter 1, Section (3), the preceding results apply to interacting charged systems if we modify the interpretation of $w(r)$ as the probability that the system is the nearest neighbor to 0 and is the center of a Debye charge cloud as well.

2. A Functional Definition and Some Notational Conventions

---

[1]R. G. Breene, Jr., Rev. Mod. Phys., 29, 94 (1957).

In order to obtain results which may readily be compared with those of Holtsmark, we shall throughout the remainder of our work measure the field $\vec{E}$ as the multiple of an n-dependent normal field $\vec{E}_n$, where

22.1 $$\vec{E} = \vec{E}_n \beta \ .$$

E_n is defined by equation (21.8) and the relation

22.2 $$E_n = \epsilon / \langle r \rangle^2 = 2.61 n^{2/3} \ .$$

We shall refer only to a monovalent-monovalent plasma, although in the general derivations use will not always be made of this fact. It will then follow that the total ion concentration is given by

22.3 $$n = 2n^{+} \ ,$$

where n^{+} represents the total density of positive ions used by Holtsmark. The probability, $W(E_o)dE_o$, for finding a field of magnitude E_o at the point O will hereafter be related to the normalized distribution function $H(\beta)$ by the equation

22.4 $$W_N(E_o)dE_o = H_N(\beta)d\beta = E_n W_N(E_o)d\beta \ .$$

Thus $H_N(\beta)$ represents $W_N(E_o)$ measured in units of the normal field strength E_n.

3. The Determination of $W(E_o)$ by the Nearest Neighbor Approximation

In the approximation,

23.1 $$W(E_o)dE_o = w(r)dr \ ,$$

consistent with the discussion of Chapter 1, Section 4, w(r) is given by the relation (21.3). The transcendental nature of expression (12.12),

23.2 $$E(r) = \frac{\epsilon Z_j(1+\kappa r)}{r^2}\exp(-\kappa r) \ ,$$

prevents the transition from the probability density, w(r), to $H(\beta)$ via

$W(E_0)$ if $H(\beta)$ is required as an explicit function of β. Consequently, β and $H(\beta)$ are obtained as parametric functions of r, using a scale factor which relates differential increments of β to those of r. Thus with the substitution of equation (22.1) into equation (23.2), there is deduced the expression

$$dr = \frac{E_n r^3 \exp(-\kappa r)}{\epsilon z_j(\kappa^2 r^2 + 2\kappa r + 2)} \, d\beta . \tag{23.3}$$

When use is made of expression (23.3), together with a comparison of equations (22.4) and (23.1), one obtains the following parametric equations:

$$\beta = \frac{(1+\kappa r)}{4.12\, n^{2/3} r^2} \exp(-\kappa r) , \tag{23.4}$$

$$H(\beta) = \frac{33.2\pi n^{5/2} r^5}{\kappa^2 r^2 + 2\kappa r + 2} \exp\left(\kappa r - \frac{4\pi r^3 n}{3}\right) . \tag{23.5}$$

$H(\beta)$ is a complicated function of temperature and total ion concentration n, which approaches the nearest neighbor approximation for Coulomb fields when the ratio n/T and with it κ tends toward zero. Typical examples are given in Figure 2. The temperature, which in most cases of physical interest does not vary by more than a factor of ten, is relatively unimportant. The difference between an ordinary Coulomb field and a shielded field can be quickly estimated from the most probable values of β. These values are smaller for the shielded field than for the Holtsmark distribution by factors lying between two and ten in the examples shown. The shape of the distribution function is distinctly different from Holtsmark's distribution.

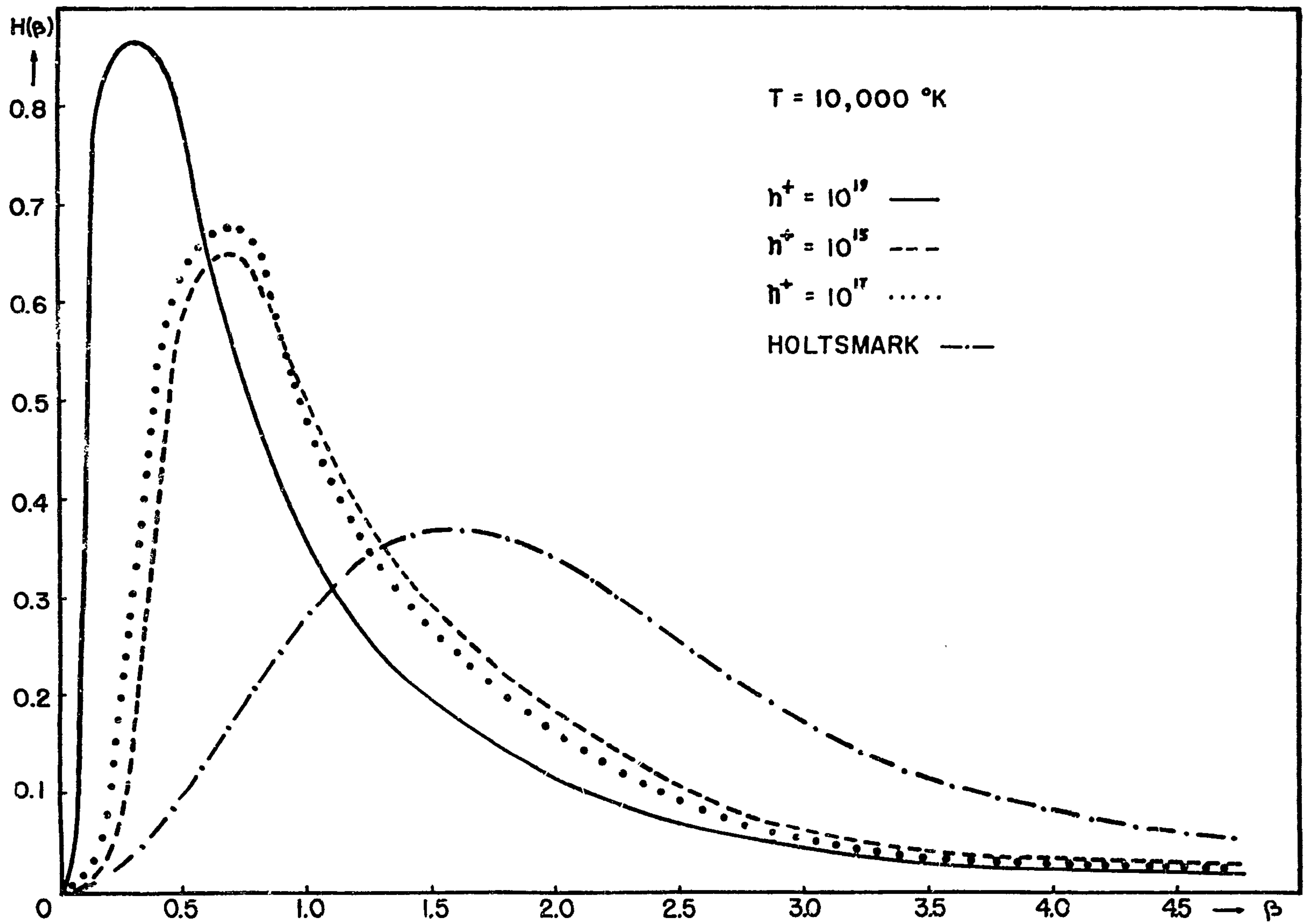

FIGURE 2 -- H(β) IN THE NEAREST NEIGHBOR APPROXIMATION

4. The Markoff Method of Summation

Markoff's[1] method is an ingenious device for summing mutually dependent probabilities whose sum has to satisfy certain auxiliary conditions. It has been discussed by various authors; notably by Holtsmark,[2] Born,[3] and Chandrasekhar.[4] The probability distribution of vector fields, e.g., the electric microfield in a plasma, represents a problem of this type. It will be fully reviewed in this section.

Denote by

24.1 $$\vec{E}_j = (X_j, Y_j, Z_j) \quad , \qquad (j = 1, 2, \ldots, N)$$

N vectors in a three dimensional space, where the components X_j, Y_j and Z_j are functions of the coordinates x_j, y_j and x_j of the source of E_j. We wish to find the probability

24.2 $$W_N(X_o, Y_o, Z_o)\,dX_o dY_o dZ_o = W_N(\vec{E}_o)\,d\vec{E}_o$$

that the resultant vector

24.3 $$\vec{E} = \sum_{j=1}^{N} \vec{E}_j(x_j, y_j, z_j) = \sum_{j=1}^{N} \vec{E}_j(\vec{r}_j)$$

has components X, Y, and Z in the intervals

24.4 $$X_o - 1/2\ dX_o \leq X \leq X_o + 1/2\ dX_o, \text{ etc.}$$

For this purpose, we introduce

---

[1] A. A. Markoff, Wahrscheinlichkeitsrechnung, Liebman, Leipzig u. Berlin (1912).

[2] J. Holtsmark, Physik. Z., 75, 73 (1924).

[3] M. Born, Optik, Springer, Berlin (1933) p. 444.

[4] S. Chandrasekhar, Rev. Mod. Phys., 15, 185 (1943).

24.5 $$\sigma_j(x_j,y_j,z_j)dx_j dy_j dz_j = \sigma_j(\vec{r}_j)d\vec{r}_j,$$

the probability that x_j, y_j and z_j lie in the ranges x_j, $x_j + dx_j$; y_j, $y_j + dy_j$; and z_j, $z_j + dz_j$ respectively. It is normalized such that

24.6 $$\int_0^\infty \sigma_j(\vec{r}_j)d\vec{r}_j = 1 , \qquad (j = 1,2,\ldots,N).$$

The distribution, $W_N(\vec{E}_o)d\vec{E}_o$, may be written

24.7 $$W_N(\vec{E}_o)d\vec{E}_o = \int \underset{3N}{\cdots} \int \prod_{j=1}^{N} \sigma_j(\vec{r}_j)d\vec{r}_j ,$$

where the integration is to be extended over those regions of the 3N dimensional configuration space $(x_1, y_1, z_1, \ldots, x_j, y_j; z_j)$ in which the inequalities (24.4) are satisfied.

This condition can be formally handled by introducing the factor

24.8 $$\Delta(\vec{r}_1,\vec{r}_2,\ldots,\vec{r}_N) = 1 \text{ whenever } X_o - 1/2dX_o \le X \le X_o + 1/2dX_o, \text{ etc.,}$$
$$\Delta(\vec{r}_1,\vec{r}_2,\ldots,\vec{r}_N) = 0 \text{ otherwise;}$$

thus transforming equation (24.7) into

24.9 $$W_N(\vec{E}_o)d\vec{E}_o = \int \underset{3N}{\cdots} \int \Delta(\vec{r}_1,\vec{r}_2,\ldots,\vec{r}_N) \prod_{j=1}^{N} \sigma_j(\vec{r}_j)d\vec{r}_j ,$$

where integration extends over the total accessible region of configuration space V.

Extension of the domain of integration to all regions of configuration space is accomplished by the formal introduction of the factor Δ . At first sight this appears to be a heuristic formalism; but it is the essence of Markoff's method that such a factor may be found.

The well known discontinuous integrals of Dirichlet δ_x, δ_y, and δ_z, of which a typical representative is

24.10 $$\delta_x = \frac{1}{\pi} \int_{-\infty}^{+\infty} \frac{\sin(\alpha_x \rho_x)}{\rho_x} \exp(i\gamma_x \rho_x) d\rho_x ,$$

have the properties

24.11 $$\begin{array}{lll} \delta_x = 1 & & -\alpha_x < \gamma_x < \alpha_x, \text{ etc.,} \\ \delta_x = 0 & & \text{otherwise.} \end{array}$$

By means of the substitutions

24.12 $$\begin{array}{llll} \alpha_x = 1/2\ dX_o, & \text{and} & \gamma_x = & \sum^N X_j - X_o; \\ \alpha_y = 1/2\ dY_o, & \text{and} & \gamma_y = & \sum^N Y_j - Y_o; \\ \alpha_z = 1/2\ dZ_o, & \text{and} & \gamma_z = & \sum^N Z_j - Z_o; \end{array}$$

into δ_x, δ_y, and δ_z respectively, it is clear that the factor

24.13 $$\Delta = \delta_x\ \delta_y\ \delta_z$$

satisfies the condition (24.8) and permits expansion of the domain of integration to include all configuration space.

The introduction of the relationships (24.10) and (24.13) into equation (24.9) yields the equality

24.14 $$W_N(\vec{E}_o)d\vec{E}_o = \frac{1}{\pi^3} \int_{3N}^{\cdots} \int \left[\prod_{j=1}^{N} \sigma_j(\vec{r}_j) \iiint_{-\infty}^{+\infty} \frac{\sin(\alpha_x \rho_x)}{\rho_x} \frac{\sin(\alpha_y \rho_y)}{\rho_y} \frac{\sin(\alpha_z \rho_z)}{\rho_z} e^{-i\vec{\gamma}\cdot\vec{\rho}} d\vec{\rho} \right] d\vec{r}_j,$$

where

24.15 $$d\vec{\rho} = d\rho_x\ d\rho_y\ d\rho_z,$$

and

24.16 $$\vec{\rho}\cdot\vec{\gamma} = \rho_x\gamma_x + \rho_y\gamma_y + \rho_z\gamma_z = |\rho||\gamma|\cos\theta.$$

Interchange of integration order gives

24.17 $$W_N(\vec{E}_o)d\vec{E}_o = \frac{1}{\pi^3} \iiint_{-\infty}^{+\infty} \int_{3N}^{\cdots} \int \frac{\sin(\alpha_x \rho_x)}{\rho_x} \frac{\sin(\alpha_y \rho_y)}{\rho_y} \frac{\sin(\alpha_z \rho_z)}{\rho_z} e^{-i\vec{\rho}\cdot\vec{\gamma}} \prod_{j=1}^{N} \sigma_j(\vec{r}_j) d\vec{r}_j\, d\vec{\rho},$$

It will be demonstrated in the succeeding development that the contribution to the integrand for absolute values of ρ greater than ten is negligible; thus justifying the approximation of sin $(\alpha\rho)$ by $\alpha\rho$ which transforms equation (24.17) into

24.18 $$W_N(\vec{E}_o)d\vec{E}_o = \frac{d\vec{E}_o}{(2\pi)^3}\iiint_{-\infty}^{+\infty} e^{-i\vec{\rho}\cdot\vec{E}_o} G_N(\rho)d\rho \ ,$$

where

24.19 $$G_N(\rho) = \int_{3N}\!\!\cdots\!\int e^{i\vec{p}\cdot(\sum_1^N \vec{E}_j)} \prod_{j=1}^{N} \sigma_j(\vec{r}_j)d\vec{r}_j .$$

The problem of finding $W(\vec{E}_o)d\vec{E}_o$ is in this manner reduced to the solutions of equations (24.18) and (24.19) by the method of Markoff. No further calculation can be made until specific forms of the vector components X_j, Y_j, Z_j, and probability densities, $\sigma_j(\vec{r}_j)$, are known. However, a case of great interest arises in many physical problems when from special symmetry properties it is known that

24.20 $$\sigma_j(\vec{r}_j)d\vec{r}_j = \sigma(\vec{r}_j)d\vec{r}_j ,$$
$$\vec{E}_j(\vec{r}_j) = \pm\vec{E}(\vec{r}_j) \ ,$$

for all values j. Equation (24.19) then may be written

24.21 $$G_N(\rho) = \left[\int_V e^{i\vec{\rho}\cdot\vec{E}} \sigma(\vec{r})d\vec{r}\right]^N$$

where integration extends over the volume V available to the sources of E.

5. The Markoff-Holtsmark Method for Evaluation of the Microfield Distribution and the Shielded Force Approximation

According to the discussion of Chapter 1, Section 4, when the nearest neighbor approximation fails, we must consider $\vec{E}_j$, the vectorial contribution to the microfield $\vec{E}_o$ of each source system. In this case the probability density of a given value $\vec{E}_o$ is proportional to the sum of those weighted sub-volumes of configuration space which are occupied by the sources. Of course, these sources are subject to the auxiliary condition that the sum of their vector contributions places $\vec{E}_o$ in a range $d\vec{E}_o$. Since this is precisely the type of problem which the Markoff method is designed to solve, the distribution function $W(\vec{E}_o)$ may be obtained immediately (at least in principle) when the probability density $\sigma_j(\vec{r}_j)$ and vector contribution $\vec{E}_j$, of each source is known.

The microfield at a point of observation 0 in a plasma may be rigorously represented as the vector sum of the Coulomb forces produced by all the point charges.

25.1 $$\vec{E} = \sum_{j=1}^{N} \vec{E}_j = \epsilon \sum_{j=1}^{N} \frac{z_j}{r_j^3} \vec{r}_j .$$

As already remarked in the introduction, Holtsmark assumed that $\sigma_j(\vec{r}_j)$ is independent of $\vec{r}_j$ and the configuration of the other charges and has the constant value $1/V$. This assumption, which is valid for non-interacting particles, simplifies the calculations decisively, but it is not admissible for systems of particles with long range interactions. However, a constant probability density $\sigma_j(\vec{r}_j)$ with the value $1/V$ can be formally used for calculating the field distribution if equation (25.1) is replaced by equation (14.1). This follows from the discussion of Chapter 1, Section 4, which showed that $\sigma_j(\vec{r}_j)$ is, in fact, equal to the volume reciprocal if the j^{th} source charge is interpreted as the center of a charge cloud; hence, as the source of a shielded Coulomb force. Thus, Holtsmark's original method can be used if, throughout, the Coulomb force is replaced by the shielded force (14.1).

For the shielded force approximation, we may determine the distribution, $W_N(\vec{E}_o)d\vec{E}_o$, by employing equation (24.18) reintroduced as

$$25.2 \qquad W_N(\vec{E}_o)d\vec{E}_o = \frac{d\vec{E}_o}{(2\pi)^3} \iiint_{-\infty}^{+\infty} e^{i\vec{\rho}\cdot\vec{E}_o} G_N(\rho)d\vec{\rho}\,.$$

Since the functional dependence upon the coordinates of a monovalent source is identical for all sources, and the probability density of any source is 1/V, equation (24.21) is applicable. It may be written as

$$25.3 \qquad G_N(\rho) = \left[\frac{1}{V}\int_V e^{i\vec{\rho}\cdot\vec{E}} d\vec{r}\right]^N ,$$

where according to equation (12.8) for a monovalent source

$$25.4 \qquad \vec{E}(r) = \pm \frac{\epsilon}{r^3}(1 + kr)e^{-kr}\vec{r}.$$

The vectorial basis for ρ has as yet been left arbitrary. If we introduce polar coordinates with polar axis along the direction of E_o, equation (25.2) is transformed to

$$25.5 \qquad W_N(\vec{E}_o)d\vec{E}_o = \frac{d\vec{E}_o}{(2\pi)^3}\int_0^\infty\int_0^\pi\int_0^{2\pi} e^{-i|\vec{\rho}||\vec{E}_o|\cos\theta} G_N(\rho)\rho^2 \sin\theta \, d\phi d\theta \, d\rho ,$$

which can be reduced to

$$25.6 \qquad W_N(\vec{E}_o)d\vec{E}_o = \frac{4\pi d\vec{E}_o}{(2\pi)^3 E_o}\int_0^\infty \rho \sin(\rho E_o)G_N(\rho)d\rho .$$

We are interested only in the absolute value of the microfield, hence in $W_N(E_o)dE_o$. It is derived by multiplying $W_N(\vec{E}_o)d\vec{E}_o$ with the appropriate weighting factor, $4\pi E_o^2$, to obtain from equation (25.6) the relation

$$25.7 \qquad W_N(E_o)dE_o = 4\pi E_o^2 W(\vec{E}_o)d\vec{E}_o = \frac{2E_o dE_o}{\pi}\int_0^\infty \rho \sin(\rho E_o)G_N(\rho)d\rho .$$

In accordance with the convention introduced in Section 2, let us further express the probability density, $W_N(E_o)$, in units of the normal field strength E_n, i.e., by introducing $H_N(\beta)$ defined in equation (22.4). Then $H_N(\beta)$ is written as

$$H_N(\beta)d\beta = E_n W_N(E_o)d\beta = \frac{2E_n^2\beta}{\pi}\, d\beta \int_0^\infty \rho \sin(E_n\beta\rho) G_N(\rho)d\rho \; ; \tag{25.8}$$

or finally,

$$H_N(\beta) = \frac{2E_n^2\beta}{\pi} \int_0^\infty \rho \sin\,(E_n\beta\rho)\; G_N(\rho)d\rho \quad , \tag{25.9}$$

where

$$G_N(\rho) = \left[\frac{1}{V}\int_V e^{i\vec{\rho}\cdot\vec{E}} \; d\vec{r}\,\right]^N \; ; \tag{25.10}$$

while β and E_n are defined by equations (22.1) and (22.2) respectively. The variable of integration ρ is a dimensionless parameter appearing via the Dirichlet integrals introduced in Section 4 of this chapter.

The evaluation of the integrals (25.9) and (25.10) constitute the complete solution to the shielded force approximation, and this problem will be considered in the following chapters.

CHAPTER III

THE LIMIT AND INTEGRATION OF THE FUNCTION $G_N(\rho)$

1. The General Properties of $G_N(\rho)$

An examination of equation (25.10) shows that $G_N(\rho)$ is a dimensionless quantity which we shall write as

31.1 $$G_N(\rho) = \left[\frac{G(\rho)}{V}\right]^N ,$$

where

31.2 $$\frac{G(\rho)}{V} = \frac{3}{4\pi R^3}\int_0^{\pi}\int_0^{2\pi}\int_0^{R} e^{i\rho|\vec{E}|\cos\theta}\, r^2 \sin\theta\, d\theta\, d\varphi\, dr .$$

The limiting form of equation (31.2) as N, V, and R tend toward infinity has certain simple properties, independent of the nature of the force law, which will first be described. From its definition, $G(\rho)$ has the dimension of a volume which is smaller than V because of the periodic nature of the integrand. Furthermore, $G(\rho)$ is only slightly smaller than V when E tends rapidly toward zero; the integrand simultaneously approaching unity as r approaches infinity. Introducing the auxiliary quantity $V^*(\rho) \ll V$, one may write

31.3 $$\left[\frac{G(\rho)}{V}\right]^N_{N\to\infty} = \left[\frac{V - V^*(\rho)}{V}\right]^N_{N\to\infty} = \left[1 - \frac{V^*(\rho)}{N/n}\right]^N_{N\to\infty} = \left[1 - \frac{g(\rho)}{N}\right]^N_{N\to\infty} = e^{-g(\rho)}$$

where n is the total concentration of charges and is equal to twice the number of positive ions. Since the probability distribution, $W(\vec{E}_o)$, of the microfield is independent of the volume of the plasma, the same must be true for $g(\rho)$ which is the only parameter in the formalism which is characteristic for the physical nature of the system. Thus $g(\rho)$ is fully determined by the force law and by the concentration, n, of point charges. For an unshielded Coulomb force, $g(\rho)$ can be rigorously calculated without using series expansions or similar approximations. A proof of this statement is given in an appendix.

In the case of a shielded force, $g(\rho)$ is a complicated function of the shielding constant κ ; hence, as in Holtsmark's work, the integral (31.2) can only be handled by numerical and graphical methods.

2. The Form of $G(\rho)/V$ in the Shielded Force Approximation

To facilitate the analysis of the function $G(\rho)/V$, it is convenient to first integrate equation (31.2) over the angles θ and φ to find

32.1 $$\frac{G(\rho)}{V} = \frac{3}{\rho R^3} \int_0^R \frac{r^2}{\rho|\vec{E}|} \sin(\rho|\vec{E}|)dr .$$

By making the substitutions

32.2 $$\eta x = (\epsilon\rho)^{1/2} \kappa x = \kappa r ,$$

32.3 $$E = \frac{\epsilon(1 + \kappa r)e^{-\kappa r}}{r^2},$$

32.4 $$F(\eta x) = (1 + \eta x)e^{-\eta x} ,$$

and

32.5 $$R^* = R/(\epsilon\rho)^{1/2},$$

one deduces that

32.6 $$\frac{G(\rho)}{V} = \frac{3}{R^{*3}} \int_0^{R^*} \frac{x^4}{F(\eta x)} \sin\left[\frac{F(\eta x)}{x^2}\right] dx .$$

For ease of reference we further put

32.7 $$I(\eta,x) = \frac{x^4}{F(\eta x)} \sin\left[\frac{F(\eta x)}{x^2}\right] ,$$

so that equation (32.6) may be written

32.8 $$\frac{G(\rho)}{V} = \frac{3}{R^{*3}} \int_0^{R^*} I(\eta,x)dx .$$

In order to analyze the integrand I we shall first study the behavior of $F(\eta x)$ and introduce an associated value of the variable x.

3. <u>The Behavior of $F(\eta x)$ and the Definition of $x_a(\eta)$</u>

An excellent approximation to $G(\rho)/V$ may be obtained through determination of its upper and lower bounds. But before doing so it is desirable to examine the behavior of $F(\eta x)$ for non-negative values of ηx, and to define a useful value for x.

Consider

33.1 $$F(\eta x) = (1 + \eta x)e^{-\eta x} \geq 0 ,$$

and

33.2 $$F'(\eta x) = -\eta x \ e^{-\eta x} \leq 0$$

for non-negative values of ηx. The function possesses a maximum at the origin and constantly decreases with increasing ηx, so that, for

33.3 $$\overline{\eta x} > \eta x ,$$

$$F(\overline{\eta x}) < F(\eta x) .$$

Let us further define $x_a(\eta)$ by the relation

33.4 $$\frac{F(\eta x_a)}{x_a^2} = a > 0 \quad .$$

Then

33.5 $$1/x_a^2 > F(\eta x_a)/x_a^2 = a,$$

and

33.6 $$x_a < a^{-1/2},$$

while

33.7 $$x_b < x_a; \quad b > a \; .$$

For convenience in the subsequent calculations it is important to have a quick method of determining $x_a(\eta)$ as a function of η when some value of "a" is specified, and consequently a nomograph may be prepared based on the following considerations.

Let the value of "a" be fixed, and write equation (33.4) as

33.8 $$a^{1/2} x_a(\eta) = \left[1 + \eta x_a(\eta)\right]^{1/2} e^{-\eta x_a(\eta)/2} \quad .$$

With "a" equal to unity,

33.9 $$x_1(\eta) = \left[1 + \eta x_1(\eta)\right]^{1/2} e^{-\eta x_1(\eta)/2} \quad .$$

Define η_a by the relation

33.10 $$\eta_a x_a(\eta_a) = \eta x_1(\eta)$$

and substitute this expression into equation (33.8). Division of the relation so obtained by equation (33.9) then yields the result

33.11 $$\frac{x_a(\eta_a)}{x_1(\eta)} = a^{-1/2} \quad ,$$

or

33.12 $$x_a(\eta_a) = a^{-1/2} x_1(\eta) \quad .$$

If equation (33.11) is substituted into equation (33.10) then

33.13 $$\eta = a^{-1/2}\,\eta_a .$$

To construct the nomograph illustrated in Figure 3, one prepares a graph of equation (33.9), and on it one also plots the linear equation (33.13) for the desired value of "a". Choosing the value η_a, the corresponding value of η is read directly. The value of x_a corresponding to η_a is then obtained by reading $x_1(\eta)$ and dividing by the square root of "a". To include in one display a sufficient range for η, the illustrated nomograph is double scaled.

4. The Geometric Character of $G(\rho)/V$

With the help of the x_a and Figure 4, the following properties of the integrand I and $G(\rho)/V$ can be easily stated:

A) $I \cong x^2$ in the interval $x_{0.1} \leq x < R^*$;

B) $0 < I < x^2$ in the interval $x_\pi < x < x_{0.1}$;

C) $$\left| \int_{x_{(m+1)\pi}}^{x_{m\pi}} I(\eta,x)dx \right| \qquad \left| \int_{x_{m\pi}}^{x_{(m-1)\pi}} I(\eta,x)dx \right| ,$$

hence the integral from zero to x_π over the oscillating part of I is negative;

D) Because of the properties listed under (C), there exists an x_a greater than x_π such that

$$\int_0^{R^*} I(\eta,x)dx = \int_{x_a}^{R^*} I(\eta,x)dx ;$$

E) In the interval $(x_a < x < x_{0.1})$, $F(\eta x)/x^2$ is less than one-tenth and greater than π, so that the sine of this function is less than the function itself. Hence, there exists an x_g in the interval

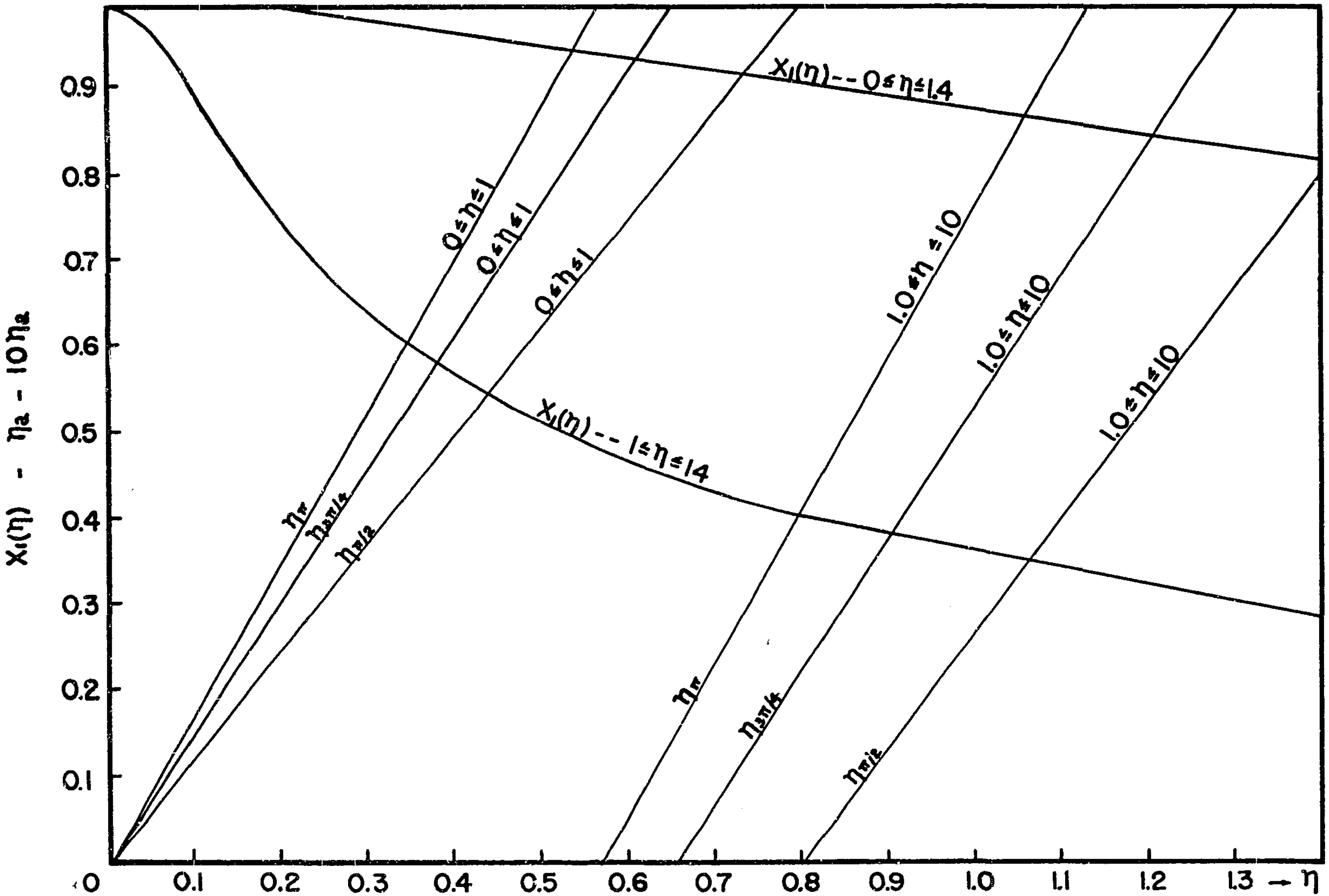

FIGURE 3 -- NOMOGRAPH FOR $X_a(\eta)$

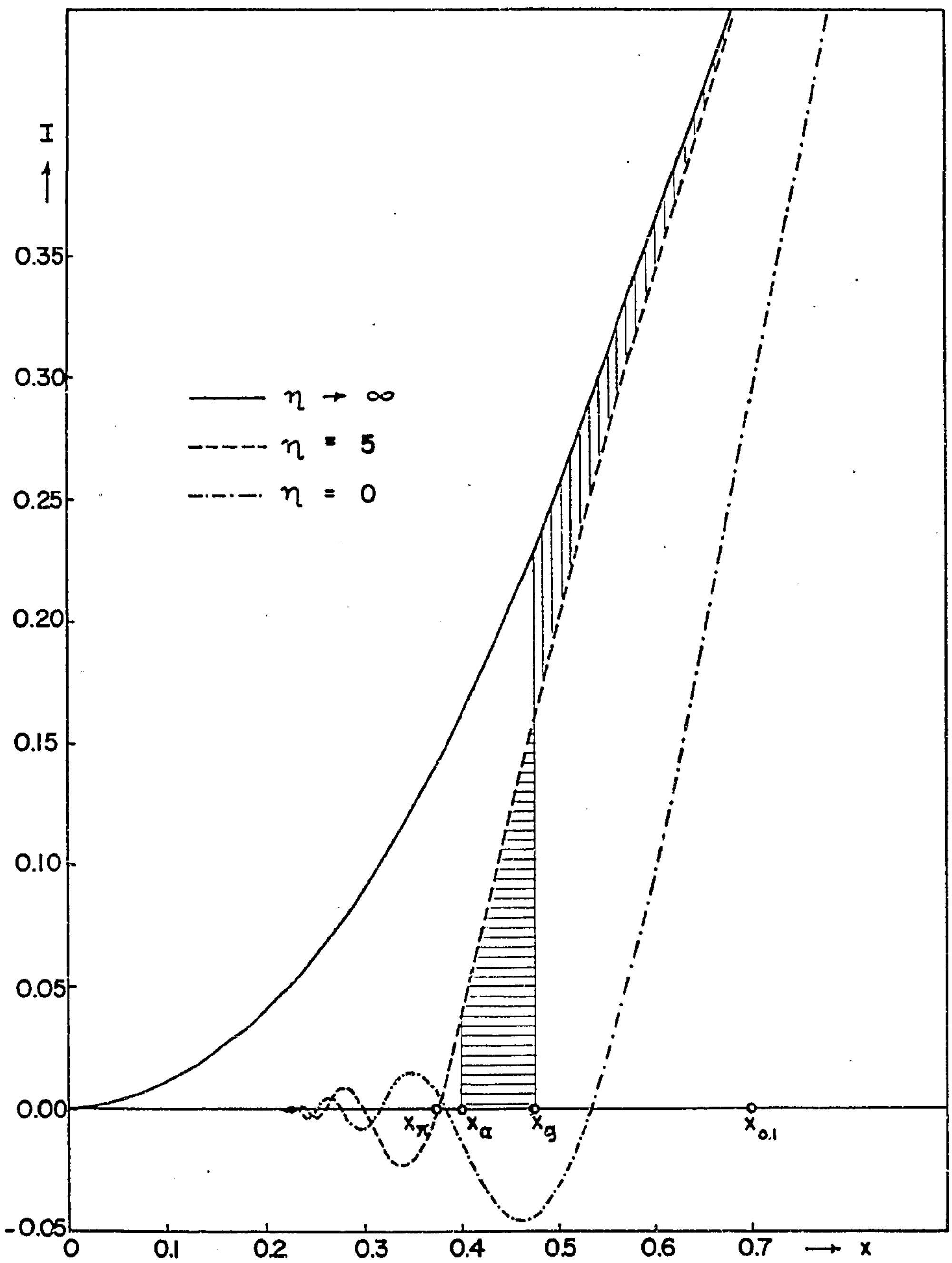

Figure 4.--The integrand I represented as a function of η. $\eta = 0$ corresponds to the unshielded Coulomb force; $\eta \to \infty$ corresponds to $I = x^2$. The characteristic parameters x_π etc., and the shaded area refer to the case $\eta = 5$.

$(x_a < x_g < x_{0.1})$ such that

$$\int_0^{R^*} I(\eta, x)dx = \int_{x_g}^{R^*} x^2 dx = \frac{1}{3}\left[R^{*3} - x_g^3\right]$$

x_g is a function of η and represents this special value of the variable x which divides the shaded area in Figure 4 into equal halves.

With the help of $x_g(\eta)$ one can write

34.1 $$\frac{G(\rho)}{V} = 1 - \frac{x_g^3(\eta)}{R^{*3}} = 1 - \frac{4\pi(\epsilon\rho)^{3/2} x_g^3(\eta)}{3V} .$$

Comparing equations (34.1) and (31.3) one finds that

34.2 $$g(\rho) = \frac{4\pi}{3} n(\epsilon\rho)^{3/2} x_g^3(\eta) .$$

Utilizing the geometrical interpretation discussed under (E), $x_g(\eta)$ and with it $g(\rho)$ can be easily estimated by graphical methods.

5. An Expression of $G(\rho)/V$ as a Sum of Integrals

Since the final integral (25.9) is rather sensitive against errors in $g(\rho)$, we shall use the more accurate method of calculating upper and lower bounds for $x_g^3(\eta)$. With slight modification, this method is adaptable for machine programing. We put

35.1 $$\frac{G(\rho)}{V} = A_1(\rho) + A_2(\rho) + A_3(\rho) ;$$

where

35.2 $$A_1(\rho) = \frac{3}{R^{*3}} \int_0^{x_\pi} I(\eta, x)dx ,$$

35.3 $$A_2(\rho) = \frac{3}{R^{*3}} \int_{x_\pi}^{x_1} I(\eta, x)dx ,$$

and

35.4 $$A_3(\rho) = \frac{3}{R^{*3}}\int_{X_1}^{R^*} I(\eta, x)dx$$

The bounds for $x_g^3(\eta)$ will be determined through examination of the functions A_1, A_2 and A_3.

6. Bounds for $A_1(\rho)$

$A_1(\rho)$ may be expressed as an infinite series by employing the notation

36.1 $$A_1(\rho) = \frac{3}{R^{*3}}\sum_{m=1}^{\infty} U_m ,$$

where

36.2 $$U_m = \int_{X_{(m+1)\pi}}^{X_{m\pi}} I(\eta, x)dx .$$

If one writes the integrand as

36.3 $$I(\eta,x) = x^2 \sin\left(\frac{F(\eta x)}{x^2}\right)\frac{x^2}{F(\eta x)} ,$$

it is clear that, for small argumental values of the sinusoidal function, $I(\eta,x)$ approaches x^2; monotonically approaching zero with x so that

36.4 $$|U_m| > |U_{m+1}| .$$

But

36.5 $$U_1 = \int_{x_{2\pi}}^{x_\pi} \frac{x^4}{F(\eta x)} \sin\frac{F(\eta x)}{x^2}\, dx ,$$

36.6 $$x_\pi \geq x \geq x_{2\pi} ,$$

36.7 $$\pi \leq F(\eta x)/x^2 \leq 2\pi ,$$

and

36.8 $$-1 \leq \sin \left[F(\eta x)/x^2\right] \leq 0.$$

It therefore follows that

36.9 $$-\frac{1}{2\pi}\int_{x_{2\pi}}^{x_{\pi}} x^2 dx < U_1 < 0 ,$$

or

36.10 $$-\frac{1}{6\pi}\left[x_{\pi}^3 - x_{2\pi}^3\right] < U_1 < 0 .$$

Combining the results (33.6), (36.4) and (36.10) it is concluded that the absolute value of each term of $A_1(\rho)$ is less than unity. The variation of the sine factor in $I(\eta, x)$ for argumental intervals of π implies that

36.11 $$U_m \leq 0 \quad \text{whenever m is odd} ,$$

and

36.12 $$U_m \geq 0 \quad \text{whenever m is even:}$$

therefore exhibiting $A_1(\rho)$ as an alternating series which meets the usual criteria for convergence and approximation. Thus,

36.13 $$\frac{3U_1}{R^{*3}} \leq A_1(\rho) \leq \frac{3(U_1 + U_2)}{R^{*3}} ,$$

and

36.14 $$\frac{1}{2\pi R^{*3}}\left[x_{\pi}^3 - x_{2\pi}^3\right] < A_1(\rho) < 0 .$$

7. Bounds for $A_2(\rho)$

For our convenience, let us divide the interval

$$x_{\pi} < x < x_1$$

into the following eleven sub-intervals:

37.1 $$\begin{array}{ll} x_{(m+1)\pi/16} \leq x \leq x_{m\pi/16} & (m = 6,7,\ldots,15) ; \\ x_{6\pi/16} \leq x \leq x_1 . & \end{array}$$

Within these respective intervals one has the corresponding relationships

37.2 $$\sin\,(m\pi/16) \leq \sin\left[F(\eta x)/x^2\right] \leq \sin\left[(m+1)\pi/16\right],$$
$$\sin\,(1) \leq \sin\left[F(\eta x)/x^2\right] \leq \sin\,(6\pi/16)\;;$$

and

37.3 $$16/(m+1)\pi \leq x^2/F(\eta x) \leq 16/m\pi\;.$$
$$16/\pi \leq x^2/F(\eta x) \leq 1\;.$$

One may now write

37.4 $$\frac{16}{6\pi}\int_{x_{6\pi/16}}^{x_1} x^2 dx + \sum_{m=6}^{15} \frac{16\sin(m\pi/16)}{(m+1)\pi}\int_{x_{(m+1)\pi/16}}^{x_{m\pi/16}} x^2 dx < \frac{R^{*3}}{3} A_2(\rho)$$

and

37.5 $$\frac{R^{*3}}{3} A_2(\rho) < \sin\,(6\pi/16)\int_{x_{6\pi/16}}^{x_1} x^2 dx + \sum_{m=6}^{15} \frac{16\sin[(m+1)\pi/16]}{m\pi}\int_{x_{(m+1)\pi/16}}^{x_{m\pi/16}} x^2 dx\;;$$

whence,

37.6 $$\frac{16\sin(1)}{6\pi R^{*3}}\left[x_1^3 - x_{6\pi/16}^3\right] + \sum_{m=6}^{15} \frac{16\sin(m\pi/16)}{(m+1)\pi R^{*3}}\left[x_{m\pi/16}^3 - x_{(m+1)\pi}^3\right] < A_2(\rho),$$

and

37.7 $$A_2(\rho) < \frac{\sin(6\pi/16)}{R^{*3}}\left[x_1^3 - x_{6\pi/16}^3\right] + \sum_{m=6}^{15} \frac{16\sin[(m+1)\pi/16]}{m\pi R^{*3}}\left[x_{m\pi/16}^3 - x_{(m+1)\pi/16}^3\right].$$

8. Bounds for $A_3(\rho)$

For calculating the limits of $A_3(\rho)$, use is made of the sinusoidal approximation

38.1 $$\alpha - \alpha^3/6 \leq \sin\alpha \leq \alpha - \alpha^3/6 - \alpha^5/120\;.$$

The left member of equation (38.1) substituted into equation (35.4) yields the relation

38.2 $$1-\frac{x^3}{R^{*3}}-\frac{1}{2R^{*3}}\int_{x_1}^{R^*}\frac{(1+\eta x)^2}{x^2}\,dx \quad < \quad A_3(\rho)\ .$$

which may be reduced to

38.3 $$1-\frac{x_1^3}{R^{*3}}-\frac{1}{2R^{*3}}\int_{x_1}^{R^*}\frac{e^{-2\eta x}}{x^2}\,dx-\frac{1}{R^{*3}}\int_{x_1}^{R^*}\frac{e^{-2\eta x}}{x}\,dx-\frac{\eta^2}{2R^{*3}}\int_{x_1}^{R^*}e^{-2\eta x}\,dx < A_3(\rho).$$

The substitution

38.4 $$V = 2\eta x$$

permits one to express equation (38.3) as

38.5 $$1-\frac{x_1^3}{R^{*3}}-\frac{\eta}{R^{*3}}\int_{2\eta x_1}^{R^*/2\eta}\left[1/v^2+1/v+1/4\right]e^{-v}\,dv \quad < \quad A_3(\rho)$$

Considering assymptotic values as R^* approaches infinity, and neglecting infinitesimals of order greater than $1/R^{*3}$, equation (38.5) may be written

38.6 $$1-\frac{1}{R^{*3}}\left[x_1^3+\frac{\eta e^{-2\eta x_1}}{4}+\frac{e^{-2\eta x_1}}{2x_1}\right] < A_3(\rho),$$

thus bounding $A_3(\rho)$ from below.

By using the right hand member of inequality (38.1), and by performing a calculation precisely as in the preceding case, there results

38.7 $$A_3(\rho) < 1-\frac{1}{R^{*3}}\left[x_1^3+\frac{\eta e^{-2\eta x_1}}{4}+\frac{e^{-2\eta x_1}}{2x_1}\right]+\frac{3}{120R^{*3}}\int_{x_1}^{R^*/2\eta}\frac{F^4(\eta x)}{x^3}\,dx.$$

For evaluation of the integral appearing in the right hand member of equation (38.7), use is made of the fact that, according to the definition of $A_3(\rho)$,

38.8 $$\eta x \geq \eta x_1\ .$$

Then

38.9 $$e^{-\eta x_1} > e^{-\eta x}$$

throughout the range of integration, which implies

38.10 $$\frac{3}{120R^{*3}}\int_{x_1}^{R^*/2\eta}\frac{F^4(\eta x)}{x^6}dx = \frac{3}{120R^{*3}}\int_{x_1}^{R^*/2\eta}\frac{(1+\eta x)^4}{x^6}e^{-4\eta x}dx < \frac{3e^{-4\eta x_1}}{120R^{*3}}\int_{x_1}^{R^*/2\eta}\frac{(1+\eta x)^4}{x^6}dx.$$

Once more by neglecting infinitesimals of order higher than $1/R^{*3}$ and considering the limit as R approaches infinity, equation (38.10) is transformed into

38.11 $$\frac{3}{120R^{*3}}\int_{x_1}^{R^*/2\eta}\frac{F^4(\eta x)}{x^6}dx < \frac{e^{-4\eta x_1}}{R^{*3}}\left[\frac{1}{200x_1^5}+\frac{\eta}{40x_1^4}+\frac{\eta^2}{20x_1^3}+\frac{\eta^3}{20x_1^2}+\frac{\eta^4}{40x_1}\right].$$

Employing the definition (33.4) for x_1, the form of equation (38.11) may be changed to read

38.12 $$\frac{3}{120R^{*3}}\int_{x_1}^{R^*/2\eta}\frac{F^4(\eta x)}{x^6}dx < \frac{x_1^3}{200R^{*3}}\left[\frac{1+5\eta x_1+10\eta^2x_1^2+10\eta^3x_1^3+4\eta^4x_1^4}{(1+\eta x_1)^4}\right].$$

$A_3(\rho)$ is now bounded from above.

9. The Bounds for $x_g^3(\eta)$ and $G(\rho)/V$

The identification of bounds to $x_g^3(\eta)$ is completed by collecting results (36.14), (37.6), (37.7), (38.6), (38.7) and (38.12). Substituting them into equation (35.1), one obtains

39.1 $$\frac{1-(\epsilon\rho)^{3/2}}{R^3}x_{gu}^3(\eta) < \frac{G(\rho)}{V} < \frac{1-(\epsilon\rho)^{3/2}}{R^3}x_{gL}^3(\eta),$$

where $x_{gu}^3(\eta)$ and $x_{gL}^3(\eta)$ are explained through the preceding operations. From equations (39.1) and (34.1) it is then deduced that

39.2 $$x_{gL}^3(\eta) < x_g^3(\eta) < x_{gu}^3(\eta)$$

and, in the limit as V and with it N approaches infinity,

$$39.3 \qquad \exp\left[\frac{4\pi n}{3}(\epsilon\rho)^{3/2} x_{gu}^{3}(\eta)\right] < \left[\frac{G(\rho)}{V}\right]_{N\to\infty}^{N} < \exp\left[\frac{4\pi n}{3}(\epsilon\rho)^{3/2} x_{gL}^{3}(\eta)\right],$$

where

$$39.4 \qquad \left[\frac{G(\rho)}{V}\right]_{N\to\infty}^{N} = \exp\left[\frac{4\pi n}{3}(\epsilon\rho)^{3/2} x_{g}^{3}(\eta)\right] .$$

Thus upper and lower bounds for the limit of $[G(\rho)/V]^N$ have been determined as functions of ρ. A graph of the functions $x_{gu}^{3}(\eta)$ and $x_{gL}^{3}(\eta)$ is given in Figure 5. Reasons advanced in the next chapter justify the omission of values for η greater than 10.

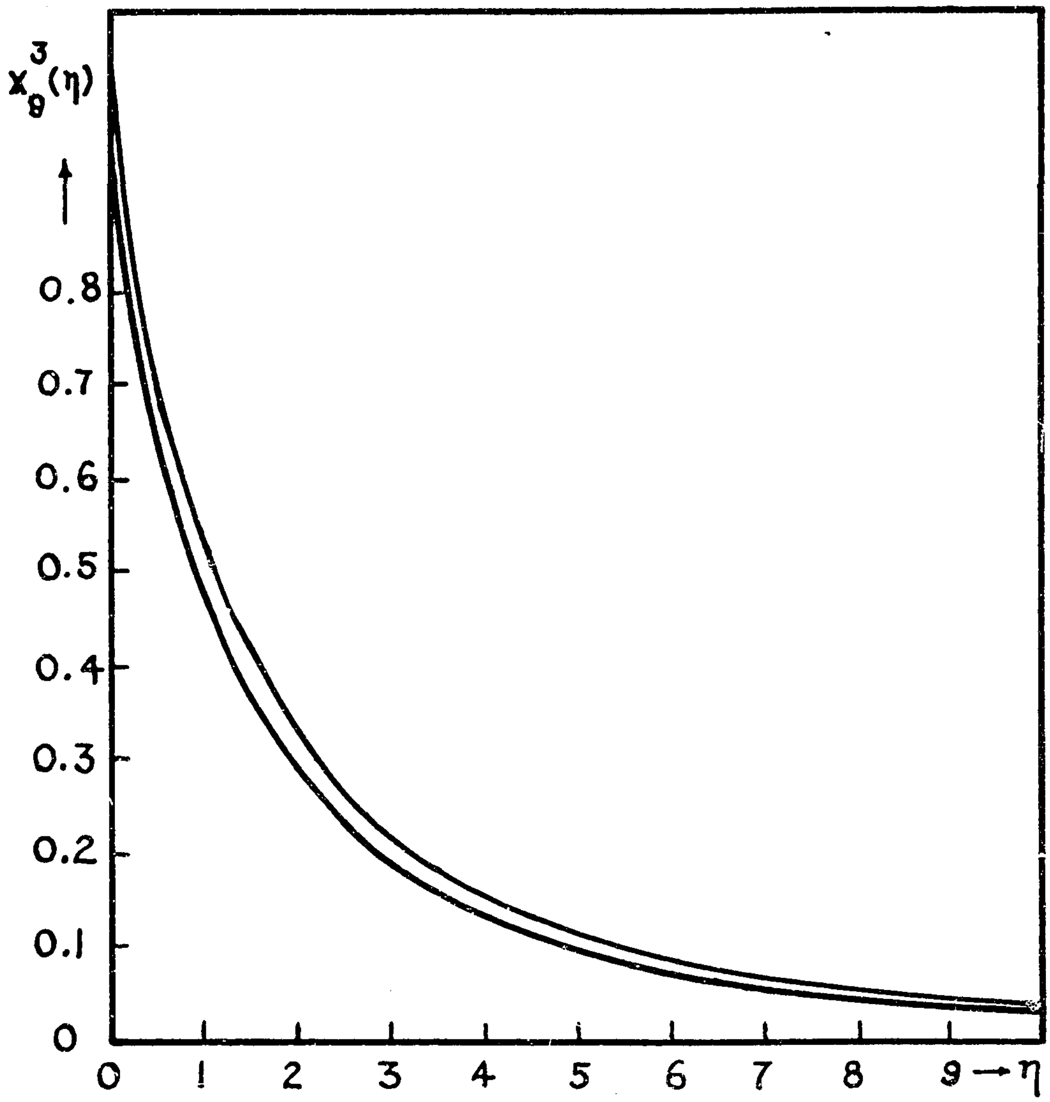

Figure 5.
Upper and Lower Limit of the Function $x_g^3(\eta)$

CHAPTER IV

THE ASSOCIATED MICROFIELD DISTRIBUTION H(β) IN THE SHIELDING FORCE APPROXIMATION

1. The Method of Evaluating H(β)

For quick reference it is useful to reintroduce the equations (25.9), (32.2), and (39.4) respectively as equations

41.1 $$H_N(\beta) = \frac{2E_n\beta}{\pi}\int_0^\infty \rho \sin(E_n\beta\rho)G_N(\rho)\,d\rho \quad ,$$

41.2 $$\eta = (\epsilon\rho)^{1/2}k \ ,$$

and

41.3 $$\lim_{N\to\infty} G_N(\rho) = \lim_{N\to\infty}\left[\frac{G(\rho)}{V}\right]^N = \exp\left[4\pi n(\epsilon\rho)^{3/2}x_g^3\right].$$

Denoting by H(β) the limiting value of $H_N(\beta)$ as N approaches infinity, substituting equation (41.3) into equation (41.1), and using the change of variable (41.2), one obtains

41.4 $$H(\beta) = \frac{4E_n^2\beta}{\pi\epsilon^2 r^2}\int_0^\infty \eta^3 \exp\left[\frac{4\pi n}{3k^3}\eta^3 x_g^3(\eta)\right]\sin\left[\frac{E_n\beta}{\epsilon k^2}\eta^2\right].$$

The function

41.5 $$\eta^3 \exp\left[\frac{4\pi n}{3k^3}\eta^3 x_g^3(\eta)\right]$$

is extremely complex, permitting only determination of upper and lower bounds. Since even these are analytically unmanagable, the integration of $H(\beta)$ is performed graphically using the bounds of expression (41.5) as envelopes for the sinusoidal function. Numerical work then shows that for values of η greater than ten (corresponding to values of ρ less than 10^{-5}) the contribution to the integral by the integrand is negligible.

To determine the profile of $H(\beta)$ an explicit choice of n and κ is made. One then plots the integrand for extremal values of $x_g^3(\eta)$ and a suitably chosen value of β. The area under the integrand is determined planimetrically. Corresponding to the extreme areal values so obtained, one finds upper and lower bounds for $H(\beta)$ for the value of β selected. A plot of the integrand of the integral (41.4) for several values of β is shown in Figure 6.

Points determined in the range β greater than three are not as reliable as those for lesser values, due to the rapid oscillation of the integrand. An aid to the profile determination is, of course, the normality of $H(\beta)$, and was employed to estimate the behavior of the distribution wing. Futhermore, the assymptotic behavior of $H(\beta)$ as β tends to infinity must be governed by the nearest neighbor of a test point and consequently is found from calculations discussed in Chapter 2, Section 3.

Since the difference between the upper and lower limit of $x_g^3(\eta)$ was smaller than the error in the graphical evaluation of $H(\beta)$, it was disregarded. The relative error in graphical integration increases with increasing field because of the numerous oscillations of the integrand of equation (41.4); it may be as large as thirty percent for β greater than two, and as large as ten percent in the region of most probable field.

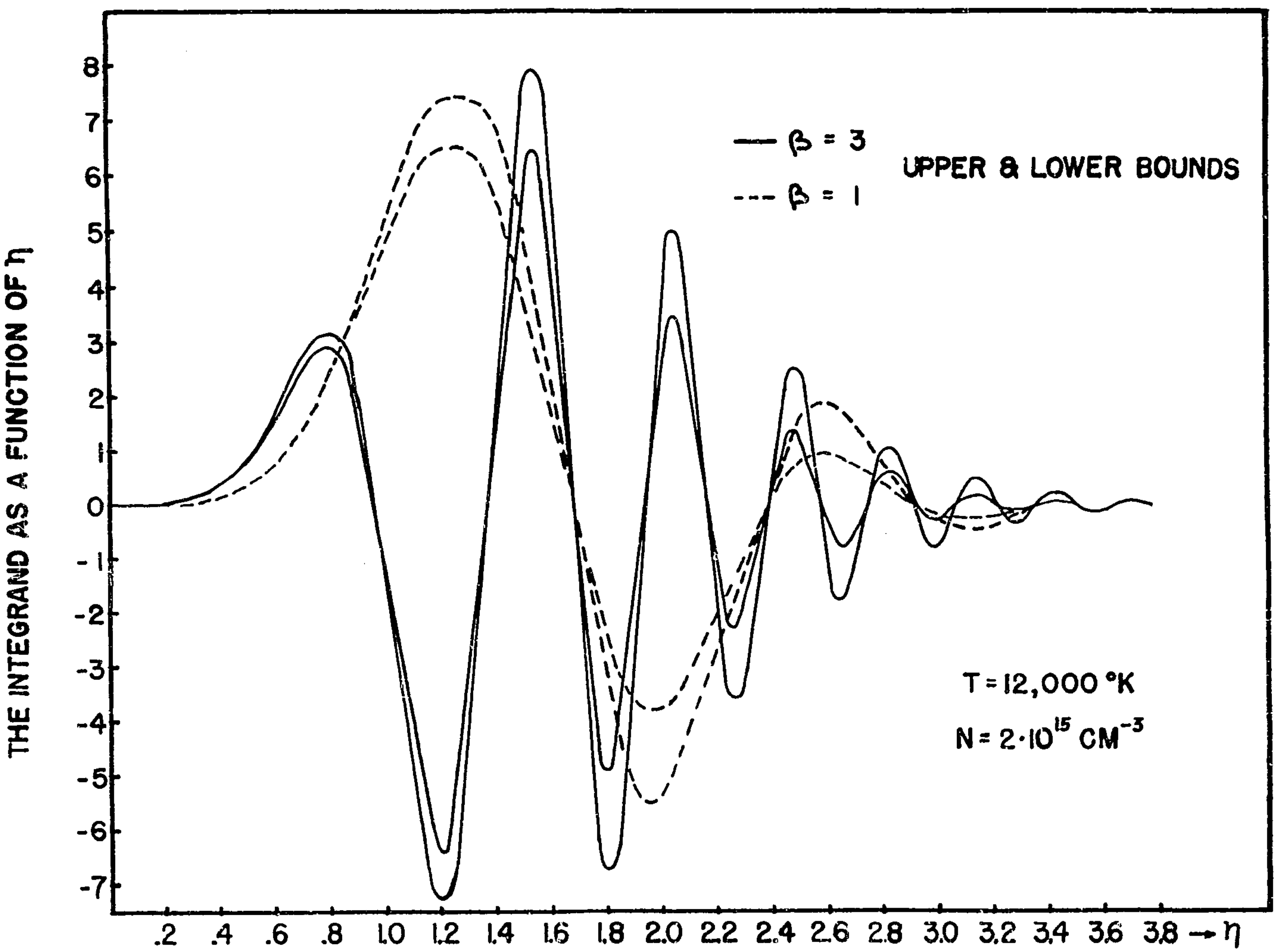

FIGURE 6 -- THE INTEGRAND OF THE FUNCTION H(β)

The profiles for $H(\beta)$ given in Figure 7 were chosen because they correspond to the situation frequently met in gas discharge tubes and stellar atmospheres.[1,2,3]

2. Discussion of Results

The curves shown in Figure 7 demonstrate the following properties of the microfield:

A). The most probable field β^* is much weaker than predicted by Holtsmark. For ion concentration of $10^{18}\mathrm{cm}^{-3}$, β^* has a value 0.3, i.e., at least five times smaller than Holtsmark's result of 1.6 for β^*. This is true over a wide range of temperature. Even for moderate ion concentrations, e.g., n approximately $10^{15}\mathrm{cm}^{-3}$, β^* is only one-half of Holtsmark's value.

For a quantitative comparison with Holtsmark's original results one has to consider that we characterise the plasma and define the normal field E_n by means of the total ion concentration n (equal to $2n^+$) of the positive and negative charge carriers. Holtsmark, on the other hand, considers only carriers of one sign and formally identifies n with n^+. This difference has physical significance when the line broadening by the microfield is investigated, since the rapidly varying electron field and the slowly varying ion field affect the line width in a different manner.

---

[1]H. Griem, Z. Physik, 137, 280 (1954).

[2]Shao-Chi Lin, E. L. Resler, and A. Kantrowitz, Jour. Applied Physics, 26, 95 (1955).

[3]G. Elstie, J. Jugaku, and L. H. Aller, Publ. of the Astron. Soc. of the Pacific, 68, 23 (1956).

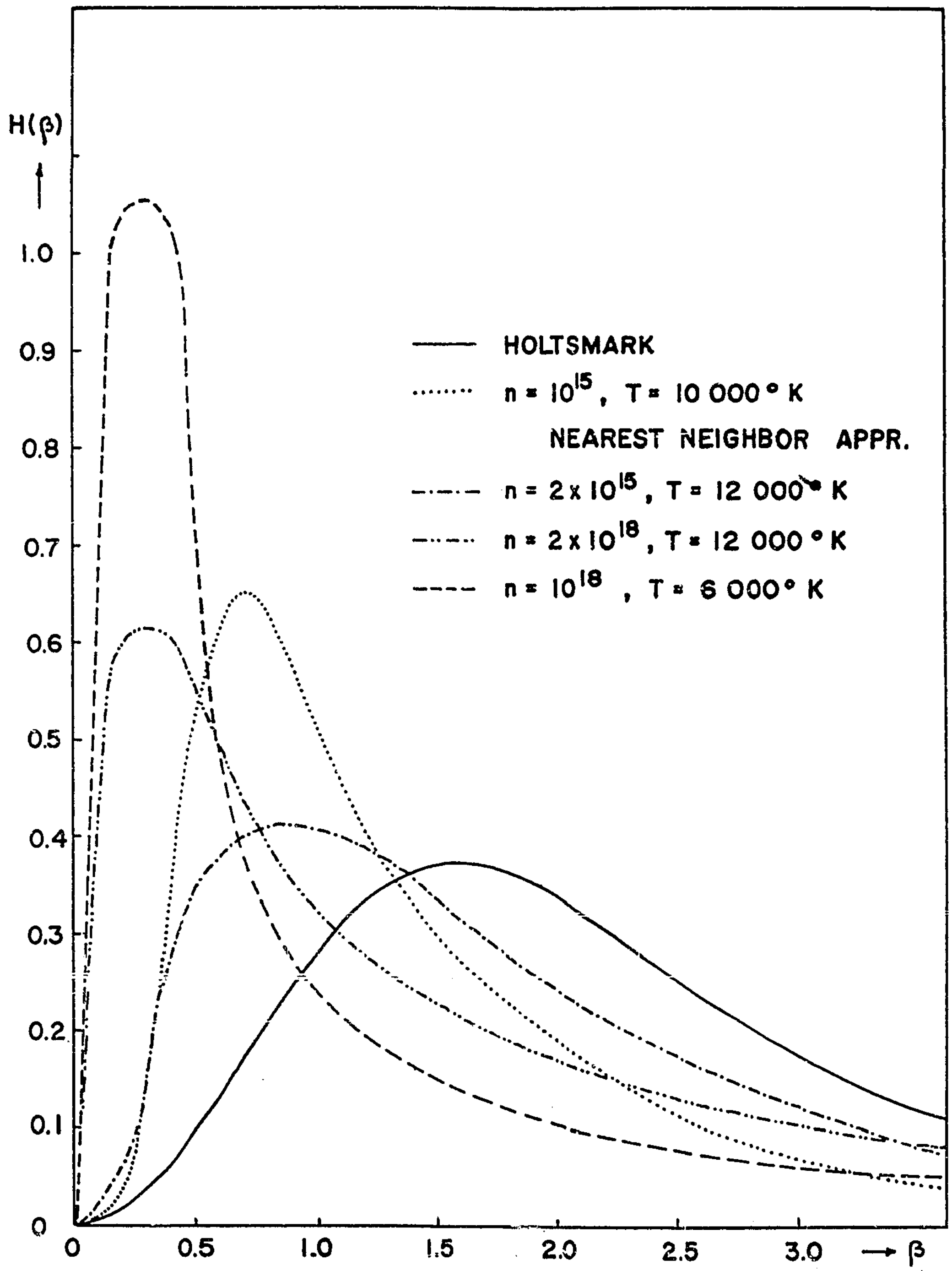

FIGURE 7.--THE DISTRIBUTION FUNCTION, $H(\beta)$

B). The half width of the distribution $H(\beta)$ is smaller than that of the Holtsmark distribution, e.g., by a factor of three for the case of an ion concentration $2 \times 10^{18} cm^{-3}$ and temperature 6,000 degrees Kelvin. This should enhance the effect of the shift of β^* on the shape of spectral lines.

C). The wings of the distribution $H(\beta)$ in regions where β is greater than unity are much lower than in the Holtsmark distribution. Formally this is a consequence of the normalization condition

42.1 $$\int_0^\infty H(\beta)d\beta = 1 ,$$

and of the fact, mentioned under (A), that the shielding effect favors weak fields. A quantitative comparison with the Holtsmark distribution is not very meaningful at present, because of the large error in computation.

D). In contrast to the simple behavior of the Holtsmark distribution, $H(\beta)$ for shielded forces is a complicated function of n. There is not only the implicit dependence via the shielding constant κ, but also an explicit correlation because of the complicated form of the force law. Thus, systems with the same κ but different n and T may differ considerably in their microfield profile. The curves for concentrations $2.10^{18} cm^{-3}$ and $10^{18} cm^{-3}$ in Figure 6 illustrate this statement.

E). All the results quoted above agree in a semi-quantitative fashion with the results obtained by the nearest neighbor approximation illustrated in Figure 2. The agreement with the latter is excellent in the case of high ion concentrations and low temperatures. For low concentration, the nearest neighbor method exaggerates the deviations from the Holtsmark distribution caused by the shielding effect (see Figure 6).

F). The shielding correction should modify the shape of spectral lines as strongly as the time dependence of the microfield which was also neglected by Holtsmark. However, the shielding effect and the velocity correction can certainly cancel each other on the wings of the spectral line. Their combined effect on the shape of spectral lines is complicated and no attempt will be made to discuss it in this thesis.

BIBLIOGRAPHY

Articles

Aller, L. H. Astrophys. J., 96, 321 (1942).

Breene, R. G., Jr. Rev. Mod. Phys., 29, 94 (1957).

Chandrasekhar, S. Rev. Mod. Phys., 15, 87 (1943).

_________, and von Neumann, J. Astrophys. J., 97, 1 (1943).

_________, Astrophys. J., 97, 255 (1943)

Debye, P., and Hückel, E. Phys. Z., 24, (1923).

Elstie, G., Jugaku, J., and Aller, L. H. Publ. of the Astron. Soc. of the Pacific, 68, 23 (1956).

Feuchtbauer, C., and Hoffmann, U. W. Ann. Physik, 43, 96 (1914).

Fowler, R. H. Proc. Camb. Phil. Soc., 22, 861 (1925).

Fowler, R. G., Atkinson, W. R., and Marks, L. W. Phys. Rev., 87, 966 (1952).

Griem, H. Z. Physik, 137, 280 (1954).

Hall, E. H. Am. Jour. of Math., 2, 287 (1879).

Hertz, P. Math. Ann., 67, 387 (1909).

Holtsmark, J. Ann. Physik, 58, 577 (1919).

_________, Physik Z., 75, 73 (1924).

Kivel, B., Bloom, S., and Margenau, H. Phys. Rev., 98, 495 (1955).

Kolb, A. C. AFOSR TN 57-8, ASTIA Document No. AD 115 040, Univ. of Mich. Eng. Res. Inst. (1956).

Kramers, H. A. Proc. Amsterdam, 30, 145 (1927).

Krogdahl, M. K. Astrophys. J., 110, 355 (1945).

Langmuir, I. Phys. Rev., 33, 954 (1929).

Lin, S., Resler, E. L., and Kantrowitz, A. Jour. Applied Physics, 26, 95 (1955).

Smoluchowski, M. Wien. Ber., 124, 577 (1915).

Spitzer, L., Jr., and Harm, R. Phys. Rev., 89, 977 (1953).

Turner, E. B., and Doherty, L. Astron. J., 60, 158 (1955).

________, AFOSR TN 56-150, ASTIA Document No. AD 86309, Univ. of Mich., Eng. Res. Inst. (1956).

Van Vleck, J. H., and Weisskopf, V. F. Rev. Mod. Phys., 17, 227 (1945).

Books

Aller, Lawrence H. The Atmospheres of the Sun and Stars. New York: Ronald Press Company, 1953.

Born, Max. Optik. Berlin: Springer, 1933.

Falkenhagen, Hans. Electrolytes. Oxford: Clarendon Press, 1934.

Markoff, A. A. Wahrscheinlichkeitsrechnung. Leipzig u. Berlin: Liebman, 1912.

Spitzer, Lyman, Jr. Physics of Fully Ionized Gases. New York: Inter-Science Publishers, Inc., 1956.

Unpublished Sources

Atkinson, W. R. "Half Intensity Breadths of the Balmer Lines in Pulsed Gas Discharges" (unpublished Master's thesis, University of Oklahoma, 1950).

Clotfelter, B. E. "Experimental Studies of Transport Phenomena in Highly Ionized Gases" (unpublished Ph.D. dissertation, University of Oklahoma, 1953).

APPENDIX

CALCULATION OF $g(\rho)$ FOR THE UNSHIELDED COULOMB FORCE

Insert the unshielded Coulomb force

A.1 $$E = z\epsilon/r^2$$

into equation (31.2), and integrate over the angular dependence. This gives

A.2 $$\frac{G(\rho)}{V} = \frac{4\pi}{V}\int_0^R \frac{r^4}{\rho} \sin(z\epsilon\rho/r^2)dr \quad .$$

Let

A.3 $$h(\rho) = \rho\,\frac{G(\rho)}{V} = \frac{4\pi}{V}\int_0^R r^4 \sin(z\epsilon\rho/r^2)dr \quad ;$$

then, if primes denote differentation with respect to ρ ,

A.4 $$h''(\rho) = -\frac{4\pi\,(z\epsilon)^{3/2}}{V}\int_0^R \sin(z\epsilon\rho/r^2)dr \quad .$$

With the new variable

A.5 $$u = z\epsilon\rho/r^2$$

equation (A.4) transforms into

A.6 $$h''(\rho) = \frac{2\pi(z\epsilon)^{3/2}\rho^{1/2}}{V}\int_\infty^{2\epsilon\rho/R^3} \frac{\sin u}{u^{3/2}}\,du \quad .$$

We consider the asymptotic expression for h'' as R approaches infinity and find

A.7
$$h''(\rho) = \frac{(2\pi z\epsilon)^{3/2}\rho^{1/2}}{V} ,$$

which integrates to

A.8
$$h(\rho) = \frac{4(2\pi z\epsilon)^{3/2}\rho^{5/2}}{15V} + c_1\rho + c_2 ;$$

or using the definition (A.3) of h

A.9
$$\frac{G(\rho)}{V} = \frac{4\pi(2\pi z\epsilon)^{3/2}}{15V}\rho^{3/2} + c_1 + c_2\rho^{-1} .$$

Since from its definition

A.10
$$\lim_{\rho\to 0}\frac{G(\rho)}{V} = 1$$

it follows that

A.11
$$c_1 = 1 , \quad c_2 = 0 .$$

Comparison of the equations (A.9) and (31.3) gives

A.12
$$g(\rho) = 4.21\, n(z\epsilon\rho)^{3/2} .$$